Synergistic effects of methylnaltrexone with 5-fluorouracil and bevacizumab on inhibition of vascular endothelial growth factor–induced angiogenesis

Patrick A. Singleton,[1] Joe G.N. Garcia,[1] and Jonathan Moss[2]

Departments of [1]Medicine and [2]Anesthesia and Critical Care, University of Chicago, Chicago, Illinois

Abstract

Many patients with cancer receive combinations of drug treatments that include 5-fluorouracil (5-FU) and bevacizumab. Therapeutic doses of 5-FU are often associated with unwanted side effects, and bevacizumab is costly. Therefore, we explored potential agents that can reduce the therapeutic concentration of these drugs. Our data indicate that methylnaltrexone (MNTX), a peripheral antagonist of the μ-opioid receptor, exerts a synergistic effect with 5-FU and bevacizumab on inhibition of vascular endothelial growth factor (VEGF)–induced human pulmonary microvascular endothelial cell (EC) proliferation and migration, two key components in cancer-associated angiogenesis. MNTX inhibited EC proliferation with an IC_{50} of ~100 nmol/L. Adding 100 nmol/L MNTX to EC shifted the IC_{50} of 5-FU from ~5 μmol/L to ~7 nmol/L. Further, adding 50 ng/mL MNTX shifted the IC_{50} of bevacizumab on inhibition of EC migration from ~25 to ~6 ng/mL. These synergistic effects were not observed with naltrexone, a tertiary μ-opioid receptor antagonist. On a mechanistic level, we observed that treatment of human EC with MNTX, but not naltrexone, increased receptor protein tyrosine phosphatase μ activity, which was independent of μ-opioid receptor expression. Silencing receptor protein tyrosine phosphatase μ expression (small interfering RNA) in human EC inhibited both synergy between MNTX and bevacizumab or 5-FU and increased VEGF-induced tyrosine phosphorylation of Src and p190 RhoGAP with enhanced activation of Akt and the actin cytoskeletal regulatory protein, RhoA, whereas silencing Src, Akt, or RhoA blocked VEGF-induced angiogenic events. Therefore, addition of MNTX could potentially lower the therapeutic doses of 5-FU and bevacizumab, which could improve index. [Mol Cancer Ther 2008;7(6):1669–79]

Introduction

Angiogenesis or the formation of new blood vessels is important in the growth and metastatic potential of various cancers. Therefore, recent therapeutic interventions for the inhibition of cancer progression include drugs that target both tumor growth and angiogenesis. Neutralizing antibodies to vascular endothelial growth factor (VEGF) including bevacizumab (Avastin) has shown promise in the treatment of metastatic renal cell cancer (1). Further, bevacizumab in combination with 5-fluorouracil (5-FU; Adrucil) and leucovorin has been used for the treatment of metastatic colorectal cancer and non-small cell lung cancer (2, 3). However, this bevacizumab and/or 5-FU regimen was often associated with unwanted side effects including venous thromboembolism, hypertension, proteinuria, and epistaxis (2–5). Therefore, agents that can reduce the therapeutic concentration of these drugs can have significant clinical utility. We recently showed that μ-opioid agonists stimulate VEGF-induced angiogenesis via receptor transactivation and that μ-opioid antagonists can inhibit VEGF receptor signaling (6). During the course of these investigations, we noted an effect of the quaternary peripheral opiate antagonist methylnaltrexone (MNTX) on endothelial cell (EC) migration and proliferation that occurred beyond the VEGF receptor. We therefore hypothesized that MNTX could have synergistic effects with antiangiogenic drugs (that is, bevacizumab and/or 5-FU).

Both opioids and VEGF stimulate Src activation required for EC proliferation and migration, two key components in angiogenesis (6). Src (pp60Src, c-Src tyrosine kinase) is a nonreceptor tyrosine kinase that contains an amino-terminal myristolyation site, Src homology sites (that is, SH2 and SH3), a tyrosine kinase catalytic domain, and regulatory tyrosine phosphorylation sites (7). Activation of Src promotes EC barrier disruption (8, 9) and EC contraction (9).

Both opioids and VEGF stimulate Src-dependent RhoA activation, which is involved in angiogenesis (10, 11). With certain angiogenic signals including VEGF, RhoA is converted from its inactive (GDP-bound) to active (GTP-bound) form via catalysis from certain Rho guanine nucleotide exchange factors (12). Further, Src can phosphorylate and inactivate the negative regulator of activated RhoA, p190 RhoGAP, which converts RhoA from its active to inactive form (13, 14). The active form of RhoA can bind to and activate other important signaling molecules

Received 10/29/07; revised 3/27/08; accepted 4/15/08.

The costs of publication of this article were defrayed in part by the payment of page charges. This article must therefore be hereby marked *advertisement* in accordance with 18 U.S.C. Section 1734 solely to indicate this fact.

Note: J. Moss serves as a paid consultant to Progenics Pharmaceuticals, has a financial interest in MNTX as a patent holder through the University of Chicago, and receives stock options from Progenics.

Requests for reprints: Jonathan Moss, Department of Anesthesia and Critical Care, University of Chicago, 5841 South Maryland Avenue, MC 4028, Chicago, IL 60637. Phone: 773-702-3901; Fax: 312-896-9187. E-mail: jm47@midway.uchicago.edu

doi:10.1158/1535-7163.MCT-07-2217

involved in angiogenesis including the serine/threonine kinase, ROCK (15).

Src activation is regulated by various processes including protein tyrosine phosphatase (PTP) activity. PTP is a diverse superfamily encoded on over 100 genes that regulate a myriad of cellular events (16). One PTP highly expressed in endothelium is the receptor PTPμ (RPTPμ; ref. 17). Structurally, RPTPμ is composed of extracellular Meprin A5 protein M-type RPTP (RPTPμ), immunoglobulin-like, and fibronectin type 3–like domains and intracellular PTP catalytic domains (18, 19). RPTPμ is localized at EC junctions and regulates vascular integrity (18, 19).

In this study, we show that MNTX acts synergistically with bevacizumab and 5-FU on inhibition of VEGF-induced angiogenic events through a μ-opioid-independent mechanism. Specifically, MNTX inhibited EC proliferation with an IC_{50} of ~100 nmol/L. Adding 100 nmol/L MNTX to EC shifted the IC_{50} of 5-FU from ~5 μmol/L to ~7 nmol/L. Further, adding 50 ng/mL MNTX shifted the IC_{50} of bevacizumab on inhibition of EC migration from ~25 to ~6 ng/mL. These synergistic effects were not observed with the uncharged μ-opioid antagonist, naltrexone. This synergistic mechanism involves MNTX activation of RPTPμ activity with consequent inhibition of VEGF (target of bevacizumab)–induced Src activation. MNTX-induced Src inactivation results in p190 RhoGAP activation and inhibition of active (GTP-bound) RhoA. Inhibition of RhoA prevents actin cytoskeletal reorganization (target of 5-FU) and consequent EC proliferation (target of 5-FU) and migration. These results suggest that addition of MNTX could potentially lower the therapeutic doses of 5-FU and bevacizumab in the treatment of various diseases exhibiting angiogenesis including cancer.

Materials and Methods

Cell Culture and Reagents

Human pulmonary microvascular EC (HPMVEC) were obtained from Cambrex and cultured as described previously (20, 21) in EBM-2 complete medium (Cambrex) at 37°C in a humidified atmosphere of 5% CO_2, 95% air, with passages 6 to 10 used for experimentation. Unless otherwise specified, reagents were obtained from Sigma. VEGF was purchased from R&D Systems. MNTX was purchased from Mallinckrodt Specialty Chemicals. Bevacizumab was purchased from Genentech. 5-FU was purchased from Abraxis Pharmaceutical Products. Reagents for SDS-PAGE electrophoresis were purchased from Bio-Rad and Immobilon-P transfer membrane was purchased from Millipore. Cytochalasin D was purchased from Calbiochem. Rabbit anti-$pSer^{473}$ Akt, rabbit anti-$pThr^{308}$ Akt, rabbit anti-Akt, and mouse anti-RPTPμ antibodies were purchased from Cell Signaling Technologies. Mouse anti-phosphotyrosine antibody, mouse anti-pp60Src antibody, and mouse anti-p190 RhoGAP antibody were purchased from Upstate Biotechnologies. Mouse anti-β-actin antibody, rabbit anti-phosphotyrosine (418) Src antibody, and naltrexone were purchased from Sigma. Secondary horseradish peroxidase–labeled antibodies were purchased from Amersham Biosciences.

Immunoprecipitation and Immunoblotting

Cellular materials from treated or untreated HPMVEC were incubated with immunoprecipitation buffer [50 mmol/L HEPES (pH 7.5), 150 mmol/L NaCl, 20 mmol/L $MgCl_2$, 1% NP-40, 0.4 mmol/L Na_3VO_4, 40 mmol/L NaF, 50 μmol/L okadaic acid, 0.2 mmol/L phenylmethylsulfonyl fluoride, 1:250 dilution of Calbiochem protease inhibitor mixture 3]. The samples were then immunoprecipitated with either anti-RPTPμ or anti-p190 RhoGAP IgG followed by SDS-PAGE in 4% to 15% polyacrylamide gels, transferred onto Immobilon membranes, and developed with specific primary and secondary antibodies. Visualization of immunoreactive bands was achieved using enhanced chemiluminescence (Amersham Biosciences).

Construction and Transfection of Small Interfering RNA against Src, RPTPμ, p190 RhoGAP, RhoA, and Akt

The small interfering RNA (siRNA) sequence(s) targeting human Src, RPTPμ, p190 RhoGAP, RhoA, and Akt1 were generated using mRNA sequences from GenBank (gi:77415509, gi:18860903, gi:150417980, gi:33876092, and gi:62241010, respectively). For each mRNA (or scramble), two targets were identified. Specifically, Src target sequence 1 (5′-AAAATCGAACCTCAGTGGCGG-3′), Src target sequence 2 (5′-AATCGAACCTCAGTGGCGGCG-3′), RPTPμ target sequence 1 (5′-AATCTGAAGGTGATGACTTCA-3′), RPTPμ target sequence 2 (5′-AACACCTTGACTAAACCGACT-3′), p190 RhoGAP target sequence 1 (5′-AAGAAAGCAAGATGTCCGAAT-3′), p190 RhoGAP target sequence 2 (5′-AAAGCAAGATGTCCGAATTCC-3′), RhoA target sequence 1 (5′-AACAGGGACTCAGGGACCAGA-3′), RhoA target sequence 2 (5′-AAATGAATGTTCCTGGGGCGC-3′), Akt1 target sequence 1 (5′-AATTATGGGTCTGTAACCACC-3′), Akt1 target sequence 2 (5′-AAATGAATGAACCAGATTCAG-3′), scrambled sequence 1 (5′-AAGAGAAATCGAAACCGAAAA-3′), and scramble sequence 2 (5′-AAGAACCCAATTAAGCGCAAG-3′) were used. Sense and antisense oligonucleotides were purchased from Integrated DNA Technologies. For construction of the siRNA, a transcription-based kit from Ambion was used (Silencer siRNA construction kit). Human lung EC were then transfected with siRNA using siPORTamine as the transfection reagent (Ambion) according to the protocol provided by Ambion. Cells (~40% confluent) were serum starved for 1 h and incubated with 3 μmol/L (1.5 μmol/L of each siRNA) of target siRNA (or scramble siRNA or no siRNA) for 6 h in serum-free medium. The serum-containing medium was then added (1% serum final concentration) for 42 h before biochemical experiments and/or functional assays were conducted.

Tyrosine Phosphatase Activity Assay

Immunoprecipitated RPTPμ from treated or untreated human pulmonary artery EC lysates was analyzed for tyrosine phosphatase activity using the fluorometric Rediplate 96 EnzChek Tyrosine Phosphatase Assay Kit (Invitrogen/Molecular Probes). Briefly, cellular materials are incubated in reaction buffer at 30°C and then added to a

96-well plate coated with 6,8-difluoro-4-methylumbelliferyl phosphate. Tyrosine phosphatase activity cleaves 6,8-difluoro-4-methylumbelliferyl phosphate into 6,8-difluoro-4-methylumbelliferyl with an excitation/emission maxima of 358/452 nm.

RhoA Activation Assay

After agonist and/or inhibitor treatment, EC are solubilized in solubilization buffer and incubated with Rho-binding domain–conjugated beads for 30 min at 4°C. The supernatant is removed and the Rho-binding domain beads with the GTP-bound form of RhoA bound are washed extensively. The Rho-binding domain beads are boiled in SDS-PAGE sample buffer and the bound RhoA material is run on SDS-PAGE, transferred to Immobilon, and immunoblotted with anti-RhoA antibody (20, 21).

HPMVEC Migration Assay

Twenty-four Transwell units with 8 μm pore size were used for monitoring *in vitro* cell migration. HPMVEC ($\sim 1 \times 10^4$ per well) were plated with various treatments (MNTX, bevacizumab, 5-FU, cytochalasin D, or siRNA) to the upper chamber and VEGF (100 nmol/L) was added to the lower chamber. Cells were allowed to migrate for 18 h. Cells from the upper and lower chamber were quantitated using the CellTiter 96 MTS assay (Promega) and read at 492 nm. Percent migration was defined as the number of cells in the lower chamber divided by the number of cells in both upper and lower chambers. Each assay was set up in triplicate, repeated at least five times, and analyzed statistically by Student's t test (with statistical significance set at $P < 0.05$).

HPMVEC Proliferation Assay

For measuring cell growth, HPMVEC (5×10^3 per well) pretreated with various agents (MNTX, bevacizumab, 5-FU, cytochalasin D, or siRNA) were incubated with 0.2 mL serum-free medium containing 100 nmol/L VEGF for 24 h at 37°C in 5% CO_2/95% air in 96-well culture plates. The *in vitro* cell proliferation assay was analyzed by measuring increases in cell number using the CellTiter 96 MTS assay (Promega) and read at 492 nm. Each assay was set up in triplicate, repeated at least five times, and analyzed statistically by Student's t test (with statistical significance set at $P < 0.05$).

HPMVEC Survival Assay

For measuring cell survival, HPMVEC (5×10^3 per well) pretreated with various agents (MNTX, bevacizumab, or 5-FU) were incubated with 0.2 mL serum-free medium containing 1 μg/mL tumor necrosis factor-α with or without 100 nmol/L VEGF for 24 h at 37°C in 5% CO_2/95% air in 96-well culture plates. The cell survival assay was analyzed by measuring the number of viable cells remaining after 24 h using the CellTiter 96 MTS assay (Promega) and read at 492 nm. Each assay was set up in triplicate, repeated at least five times, and analyzed statistically by Student's t test (with statistical significance set at $P < 0.05$).

Immunofluorescence Microscopy and F-Actin Cytoskeleton Quantitation

Polymerized actin rearrangement was assessed with Texas red–conjugated phalloidin (Invitrogen/Molecular Probes) and analyzed using a Nikon Eclipse TE 300 microscope as we have described (22). Computer recorded .tiff images were analyzed with ImageQuant software from Amersham Biosciences. A standardized average gray value was generated for total phalloidin staining versus total cellular area for each cell (20). To calculate percent F-actin staining per cell, the following equation was used: [(total F-actin standardized average gray value) / (total cellular area)] × 100. Fifty cells per condition were analyzed.

Statistical Analysis

Student's t test was used to compare the mean from two or more different experimental groups. Results are expressed as mean ± SE.

Results

Analysis of MNTX Synergy with Bevacizumab and 5-FU on Inhibition of EC Proliferation and Migration

Bevacizumab treatment of cancer is costly and the therapeutic doses of 5-FU are often associated with unwanted side effects (4, 23–28). Therefore, agents that can reduce the therapeutic concentration of these drugs can have significant clinical utility. Our recent published data indicate that the peripheral μ-opioid receptor antagonist, MNTX, inhibits opiate and VEGF-induced angiogenesis via inhibition of VEGF receptor signaling (6). We therefore hypothesized that MNTX could have synergistic effects with antiangiogenic drugs (that is, bevacizumab and/or 5-FU). Figure 1A indicates that MNTX inhibits EC proliferation with an IC_{50} of ~100 nmol/L. Adding 100 nmol/L MNTX to EC shifted the IC_{50} of 5-FU from ~5 μmol/L to ~7 nmol/L. Further, adding 50 ng/mL MNTX shifted the IC_{50} of bevacizumab on inhibition of EC migration from ~25 to ~6 ng/mL (Fig. 1B). These synergistic effects were not observed with the uncharged μ-opioid antagonist, naltrexone (Fig. 1C and D). Further, we observed a synergistic effect of MNTX with a combination of bevacizumab and 5-FU on inhibition of VEGF-induced proliferation, migration, and survival (Fig. 2A).

Roles of Src and Akt in MNTX, Bevacizumab, and 5-FU Inhibition of VEGF-Induced Angiogenesis

We next examined the mechanism(s) of the synergistic effects of MNTX with bevacizumab and 5-FU on inhibition of VEGF-induced angiogenic events. Our previous published data indicate that Src activation is important in VEGF-induced angiogenesis (6). Figure 2B indicates that MNTX and bevacizumab, but not 5-FU or naltrexone, inhibit VEGF-induced Src activation (tyrosine phosphorylation). MNTX inhibits Src activation with an IC_{50} of ~5 nmol/L (Fig. 2B). We and others have reported that the serine/threonine kinase Akt regulates cellular migration and proliferation (29). Figure 2C indicates that MNTX, bevacizumab, and 5-FU inhibit VEGF-induced Akt activation (serine/threonine phosphorylation). MNTX inhibits Akt activation with an IC_{50} of ~10 nmol/L (Fig. 2C). Both Src and Akt activation can regulate actin cytoskeletal dynamics (13). Silencing Src or Akt expression (siRNA) or inhibiting actin cytoskeletal reorganization (cytochalasin D)

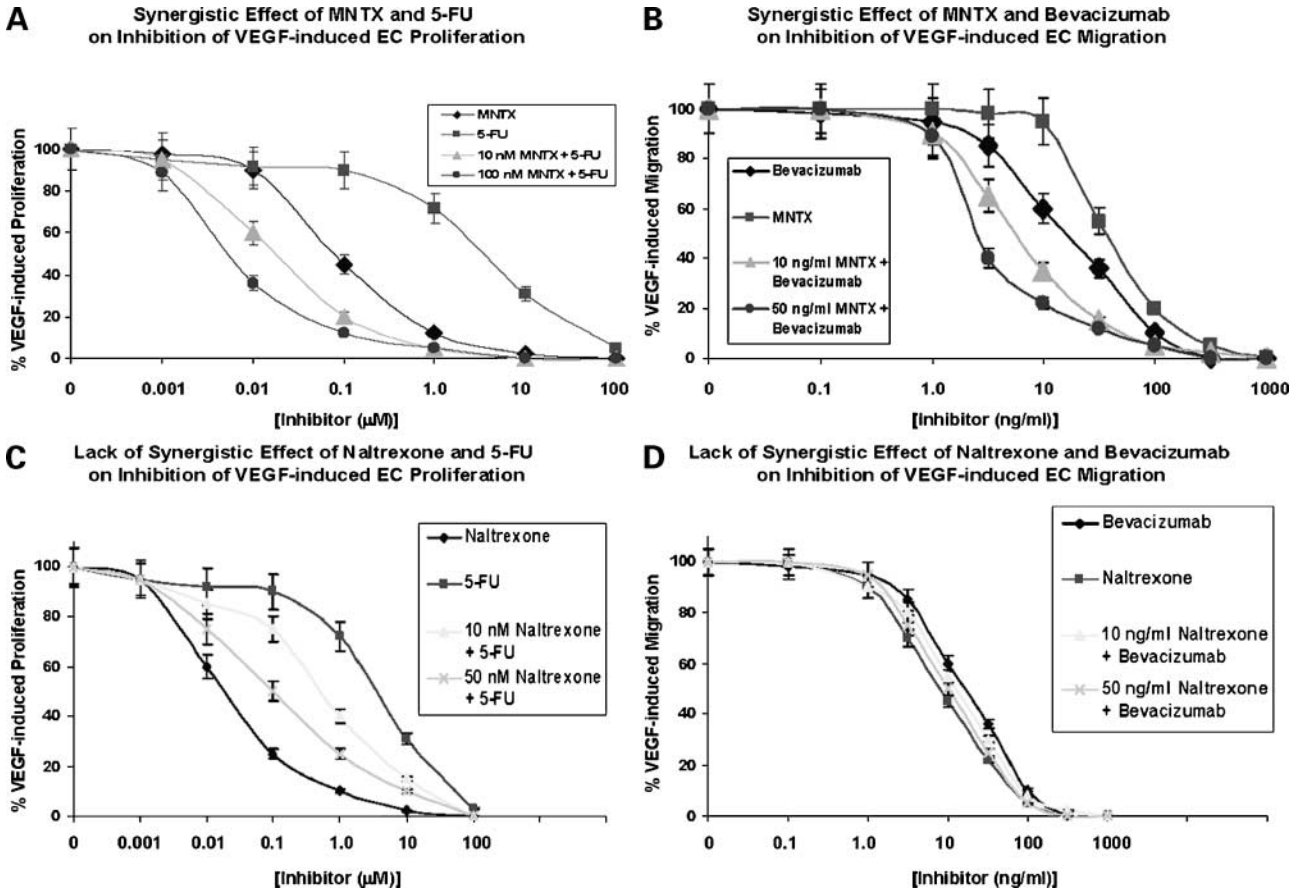

Figure 1. Determination of MNTX synergistic effects with bevacizumab and 5-FU on inhibition of VEGF-induced EC proliferation and migration. **A,** graphical representation of human EC assayed for VEGF (100 nmol/L) – induced proliferation (24 h) in the presence or absence of 0.001, 0.01, 0.1, 1.0, 10, or 100 μmol/L MNTX, 5-FU, 5-FU + 10 nmol/L MNTX, or 5-FU + 100 nmol/L MNTX. Experiments were done in triplicate. *Bars,* SD. **B,** graphical representation of human EC assayed for VEGF (100 nmol/L) – induced migration (24 h) in the presence or absence of 0.1, 1.0, 10, 100, or 1,000 ng/mL MNTX, bevacizumab, bevacizumab + 10 ng/mL MNTX, or bevacizumab + 50 ng/mL MNTX. The unit ng/mL was used instead of μmol/L due to the proprietary nature of the molecular weight of bevacizumab. Experiments were done in triplicate. *Bars,* SD. **C,** graphical representation of human EC assayed for VEGF (100 nmol/L) – induced proliferation (24 h) in the presence or absence of 0.001, 0.01, 0.1, 1.0, 10, or 100 μmol/L naltrexone, 5-FU, 5-FU + 10 nmol/L naltrexone, or 5-FU + 100 nmol/L naltrexone. Experiments were done in triplicate. *Bars,* SD. **D,** graphical representation of human EC assayed for VEGF (100 nmol/L) – induced migration (24 h) in the presence or absence of 0.1, 1.0, 10, 100, or 1,000 ng/mL naltrexone, bevacizumab, bevacizumab + 10 ng/mL naltrexone, or bevacizumab + 50 ng/mL naltrexone. The unit ng/mL was used instead of μmol/L due to the proprietary nature of the molecular weight of bevacizumab. Experiments were done in triplicate. *Bars,* SD.

blocked VEGF-induced EC proliferation and migration (Fig. 2D).

Role of RPTPμ in MNTX, Bevacizumab, and 5-FU Inhibition of VEGF-Mediated Angiogenesis

Our results from Fig. 2 indicate that MNTX blocks VEGF-induced pp60Src activation (tyrosine phosphorylation). One possible mechanism of attenuating Src tyrosine phosphorylation is through regulation of tyrosine phosphatase activity. An important tyrosine phosphatase implicated in regulating human pulmonary EC contacts is the RPTPμ (18, 19). MNTX, but not naloxone, treatment of HPMVEC enhanced RPTPμ tyrosine phosphatase activity (Fig. 3A). In addition, VEGF inhibits and MNTX promotes RPTPμ complex formation with Src (Fig. 3B). Further, silencing RPTPμ (Fig. 3B) prolonged VEGF-induced Src tyrosine phosphorylation, whereas silencing Src inhibited Akt activation (Fig. 3C and D).

Because Src and Akt can regulate the actin cytoskeleton and actin cytoskeletal reorganization is required for VEGF-induced angiogenic events (Fig. 2D), we next examined F-actin dynamics in human EC using TRITC-tagged phalloidin. Figure 4A indicates that VEGF increases total phalloidin staining per EC. These effects are inhibited by MNTX, bevacizumab, or 5-FU treatment of human EC. Further, silencing Src expression inhibited VEGF-induced increase in F-actin, whereas silencing RPTPμ expression enhanced F-actin staining.

Role of p190 RhoGAP and RhoA in MNTX, Bevacizumab, and 5-FU Inhibition of VEGF-Mediated Angiogenesis

Our results from Figs. 2, 3, and 4A indicate that Src-mediated actin cytoskeletal dynamics are important in VEGF-induced EC proliferation and migration and MNTX inhibits these effects through RPTPμ activation. The small

G protein, RhoA, is a crucial regulator of VEGF-induced actin cytokeletal reorganization and consequent angiogenic events (10). We therefore examined the regulation of RhoA activation by MNTX and RPTPμ.

With certain angiogenic signals including VEGF, RhoA is converted from its inactive (GDP-bound) to active (GTP-bound) form via catalysis from certain Rho guanine nucleotide exchange factors (12). Further, Src can phosphorylate and inactivate the negative regulator of activated RhoA, p190 RhoGAP, which converts RhoA from its active to inactive form (13, 14). Figure 4B indicates that VEGF induces tyrosine phosphorylation of p190 RhoGAP in human EC. Silencing Src blocks this tyrosine phosphorylation, whereas silencing RPTPμ enhances it. Further, MNTX and bevacizumab (but not 5-FU) treatment of human EC blocks VEGF-induced RhoA activation (Fig. 4C). Finally, silencing Src blocks VEGF-induced RhoA activation, whereas silencing RPTPμ or p190 RhoGAP enhances VEGF-induced RhoA activation (Fig. 4D).

The importance of RPTPμ-mediated RhoA regulation on MNTX synergistic inhibition of VEGF-induced angiogenic events is shown in Fig. 5. Silencing RPTPμ or p190 RhoGAP enhances, whereas silencing RhoA inhibits, VEGF-induced EC proliferation and migration (Fig. 5A and B). Silencing RPTPμ attenuates MNTX inhibition of EC proliferation (shift of IC_{50} from ~100 nmol/L to 10 μmol/L) and migration (shift in IC_{50} from ~50 to ~300 ng/mL; Fig. 5C and D). Further, silencing RPTPμ blocks the synergistic effects of MNTX with 5-FU on inhibition of VEGF-induced EC proliferation as indicated by the shift in the IC_{50} from ~7 nmol/L to ~6 μmol/L (Fig. 5C). Further, silencing RPTPμ blocks the synergistic effects of MNTX with bevacizumab on inhibition of VEGF-induced EC migration as indicated by the shift in the IC_{50} from ~6 to ~30 ng/mL (Fig. 5D).

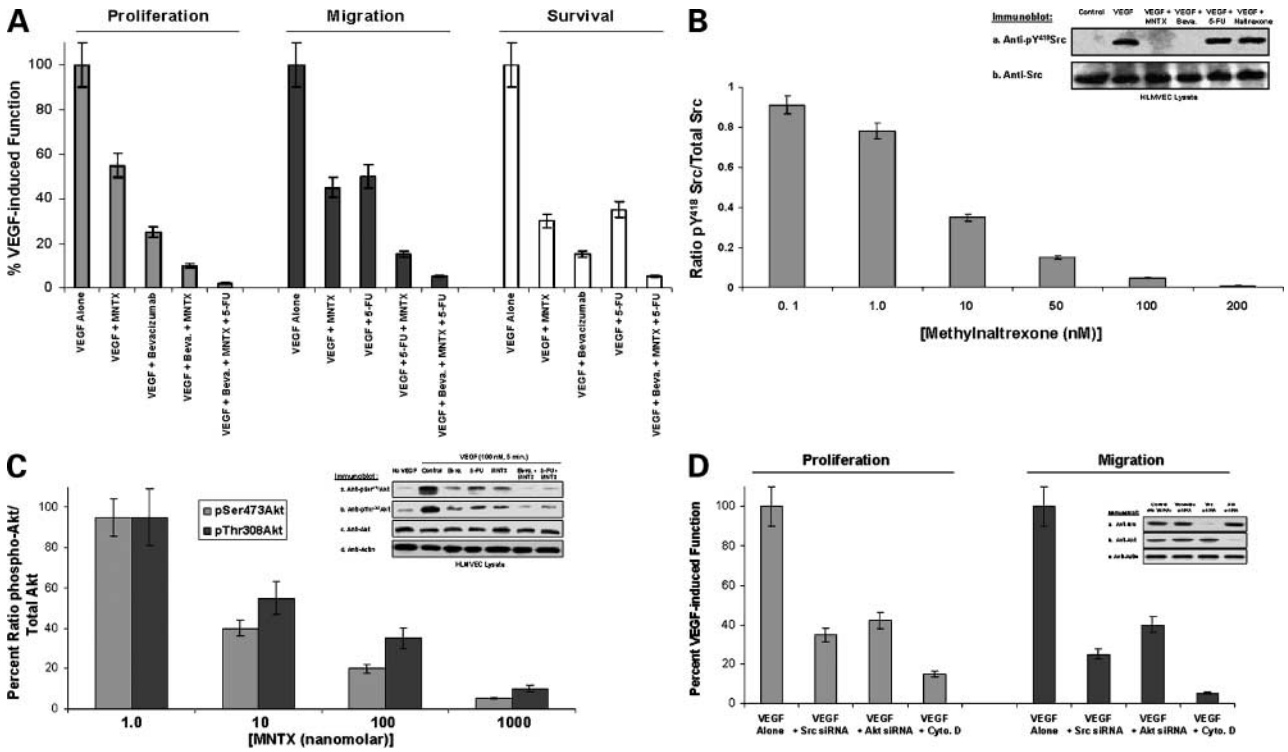

Figure 2. Analysis of MNTX, bevacizumab, and 5-FU regulation of VEGF-induced Src and Akt activation in human EC. **A,** graphical representation of VEGF (100 nmol/L) – induced human EC proliferation, migration, or survival (protection from tumor necrosis factor-α – mediated EC death) in the absence or presence of pretreatment with 100 nmol/L MNTX, 5 μmol/L 5-FU, and 25 ng/mL bevacizumab alone or in combination as described in Materials and Methods. **B,** graphical representation of the effects of various concentrations of MNTX (0.1, 1.0, 10, 50, 100, and 200 nmol/L) on inhibition of VEGF-induced Src activation. *Y axis,* ratio of pY^{418} Src immunoreactive band intensity divided by total Src immunoreactive band intensity as described in Materials and Methods. *Inset,* human EC were serum starved for 1 h and either untreated (control) or treated with VEGF (100 nmol/L, 5 min) with or without pretreatment (1 h) with 100 nmol/L MNTX, 100 ng/mL bevacizumab, 100 μmol/L 5-FU, or 100 nmol/L naltrexone. EC lysates were obtained, run on SDS-PAGE, and immunoblotted with anti-pY^{418} Src (*a*) or anti-Src (*b*) antibody. **C,** graphical representation of the effects of various concentrations of MNTX (1.0, 10, 100, and 1,000 nmol/L) on inhibition of VEGF-induced Akt activation. *Y axis,* ratio of $pSer^{473}$ Akt or $pThr^{308}$ Akt immunoreactive band intensity divided by total Akt immunoreactive band intensity as described in Materials and Methods. *Inset,* human EC were serum starved for 1 h and either untreated (control) or treated with VEGF (100 nmol/L, 5 min) with or without pretreatment (1 h) with 100 nmol/L MNTX, 100 ng/mL bevacizumab, or 100 μmol/L 5-FU. EC lysates were obtained, run on SDS-PAGE, and immunoblotted with anti-$pSer^{473}$ Akt (*a*), anti-$pThr^{308}$ Akt (*b*), anti-Akt (*c*), or anti-actin (*d*) antibody. **D,** graphical representation of VEGF (100 nmol/L) – induced human EC proliferation or migration in the absence or presence of pretreatment with Src siRNA, Akt siRNA, or cytochalasin D (10 μmol/L). *Inset,* human EC either untreated (control) or treated with scramble siRNA, Src siRNA, or Akt1 siRNA for 48 h. Lysates were obtained, run on SDS-PAGE, and immunoblotted with anti-Src (*a*), anti-Akt (*b*), or anti-actin (*c*) antibody.

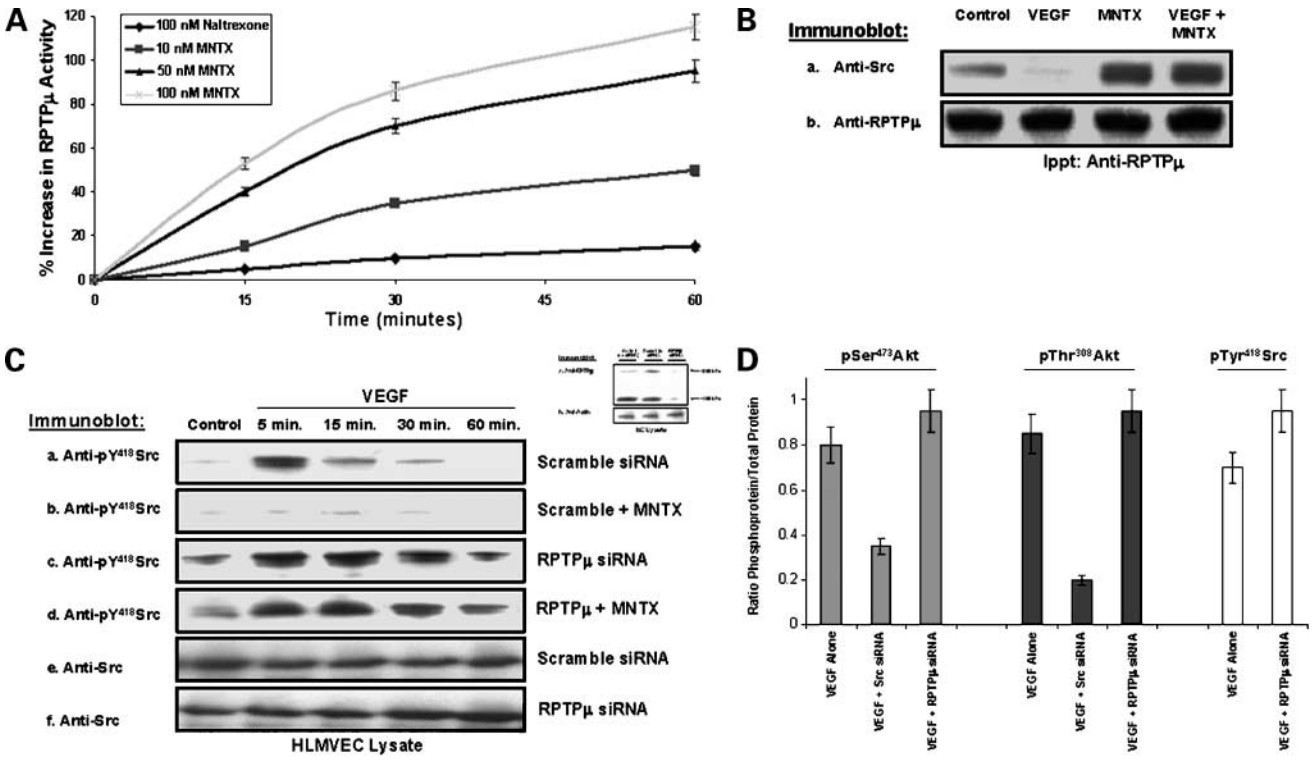

Figure 3. Determination of MNTX regulation of RPTPμ activity and RPTPμ-mediated Src inhibition in human EC. **A,** human EC were serum starved for 1 h and either untreated or treated with 10, 50, or 100 nmol/L MNTX or 100 nmol/L naltrexone for 1 h. EC were then solubilized in immunoprecipitation buffer [50 mmol/L HEPES (pH 7.5), 150 mmol/L NaCl, 20 mmol/L $MgCl_2$, 1% NP-40, 0.2 mmol/L phenylmethylsulfonyl fluoride, 1:250 dilution of Calbiochem protease inhibitor mixture 3] and immunoprecipitated with anti-RPTPμ antibody. Tyrosine phosphatase activity measurements were done on the immunobeads for 0, 15, 30, and 60 min as described in Materials and Methods. *Y axis,* percent increase in RPTPμ activity over control, with control being RPTPμ isolated from untreated EC. Each experiment was done in triplicate. *Bars,* SD. **B,** human EC were either untreated (control) or treated with 100 nmol/L VEGF for 5 min and pretreated with 100 nmol/L MNTX for 1 h or both. EC were then solubilized in immunoprecipitation buffer [50 mmol/L HEPES (pH 7.5), 150 mmol/L NaCl, 20 mmol/L $MgCl_2$, 1% NP-40, 0.2 mmol/L phenylmethylsulfonyl fluoride, 1:250 dilution of Calbiochem protease inhibitor mixture 3] and immunoprecipitated with anti-RPTPμ antibody. The immunoprecipitated material was run on SDS-PAGE and immunoblotted with anti-Src (*a*) or anti-RPTPμ (*b*) antibody. **C,** human EC were serum starved for 1 h and either untreated (control) or treated with 100 nmol/L VEGF for 5, 15, 30, or 60 min with pretreatment with scramble siRNA (siRNA that does not target any known mRNA sequence) or RPTPμ siRNA. EC lysates were obtained, run on SDS-PAGE, and immunoblotted with anti-pY^{418} Src (*a-d*) or anti-Src (*e* and *f*) antibody. Experiments were done in triplicate. Representative data are shown. *Inset,* human EC either untreated (control) or treated with scramble siRNA or RPTPμ siRNA for 48 h. Lysates were obtained, run on SDS-PAGE, and immunoblotted with anti-RPTPμ (*a*) or anti-actin (*b*) antibody. **D,** graphical representation of the effects of silencing Src or RPTPμ expression on VEGF-induced Akt or Src activation (phosphorylation). *Y axis,* ratio of $pSer^{473}$ Akt or $pThr^{308}$ Akt immunoreactive band intensity divided by total Akt immunoreactive band intensity or the ratio of pY^{418} Src immunoreactive band intensity divided by total Src immunoreactive band intensity as described in Materials and Methods.

Discussion

We and others have noted previously an effect of opiates on EC migration and proliferation, and an effect of opiate antagonists in attenuating opiate-induced angiogenesis (5). In this study, we present the novel findings that MNTX, a selective peripheral antagonist of the μ-opioid receptor, acts in a synergistic manner with bevacizumab and 5-FU in inhibiting VEGF-induced angiogenic events through a μ-opioid-independent mechanism, which involves activation of RPTPμ. Our results suggest that the synergistic effects of MNTX with bevacizumab and 5-FU are achieved through inhibition of different components of a common VEGF-induced angiogenic signaling pathway. Bevacizumab inhibits the initial VEGF binding to VEGF receptors. MNTX stimulation of RPTPμ activity inhibits VEGF-induced Src activation, Src-mediated p190 RhoGAP inactivation (tyrosine phosphorylation), and consequent RhoA activation. 5-FU inhibits VEGF-induced Akt activation and actin cytoskeletal reorganization. Inhibition of these events promotes synergistic inhibition of VEGF-induced EC proliferation and migration (angiogenesis; Fig. 6). Therefore, we hypothesize that, in addition to its effects on gastrointestinal motility, MNTX might have clinical utility by potentially lowering the therapeutic doses of 5-FU and bevacizumab in the treatment of various diseases requiring angiogenesis including cancer.

The μ-opioid antagonist, naloxone, is fairly lipid soluble and crosses the blood-brain barrier easily (30–32). Despite numerous attempts at regulating doses, μ-opioid antagonists have proven unsuitable for patients receiving opiates for pain management because of analgesia reversal and breakthrough pain (33). MNTX is a quaternary derivative of the tertiary μ-opiate antagonist naltrexone (34). The addition of the methyl group to naltrexone at the amine

in the ring forms the compound *N*-MNTX with greater polarity and lower lipid solubility. Because MNTX does not cross the blood-brain barrier, it could play a therapeutic role in reversing the peripheral effects of opiates in palliative care, especially for patients taking high doses of opiates for analgesia (35). Two recently completed phase III double-blind clinical trials of s.c. MNTX in patients with advanced illness suffering from opiate-induced constipation showed significant reversal of constipation without affecting analgesia (30, 34, 36). Doses of MNTX used clinically were 0.15 or 0.3 mg/kg s.c. (37). The FDA recently approved Relistor (methylnaltrexone) to help restore bowel function in patients with late-stage, advanced illness and who are receiving opioids on a continous basis to help alleviate their pain (FDA.gov, April 24, 2008). Oral MNTX has shown activity in volunteer studies, although at much higher doses (35). Additionally, MNTX might play a role in oncologic surgery as it is currently in phase III trials for postoperative ileus (37). Additionally, there is evidence that delayed gastric emptying is a peripheral effect of opiates and is reversible by MNTX (30, 34, 36). These findings suggest that MNTX may have a clinical role in the perioperative period, the intensive care unit, or with advanced illness. Because the advanced illness population of patients likely to receive MNTX is composed predominantly of patients with cancer, we have focused our study on MNTX rather than the tertiary opiate antagonists, which are rarely used in these populations.

Although we have not done any *in vivo* angiogenesis studies of MNTX, we note that the plasma concentrations of opiates, MNTX, and chemotherapeutic agents reported from various clinical trials seem well within the range of the effects that we have described in our current *in vitro* study. Peak plasma concentrations of i.v. or i.m. morphine in normal therapeutic doses are 80 ng/mL (38). In one comprehensive review (39), analgesia in cancer patients was associated with steady-state concentrations of morphine in plasma ranging from 6 to 364 ng/mL. A meta-analysis of dose-adjusted peak plasma concentrations of morphine revealed a C_{max} of 1 to 10 nmol/L per L/mg morphine, although there were some differences between

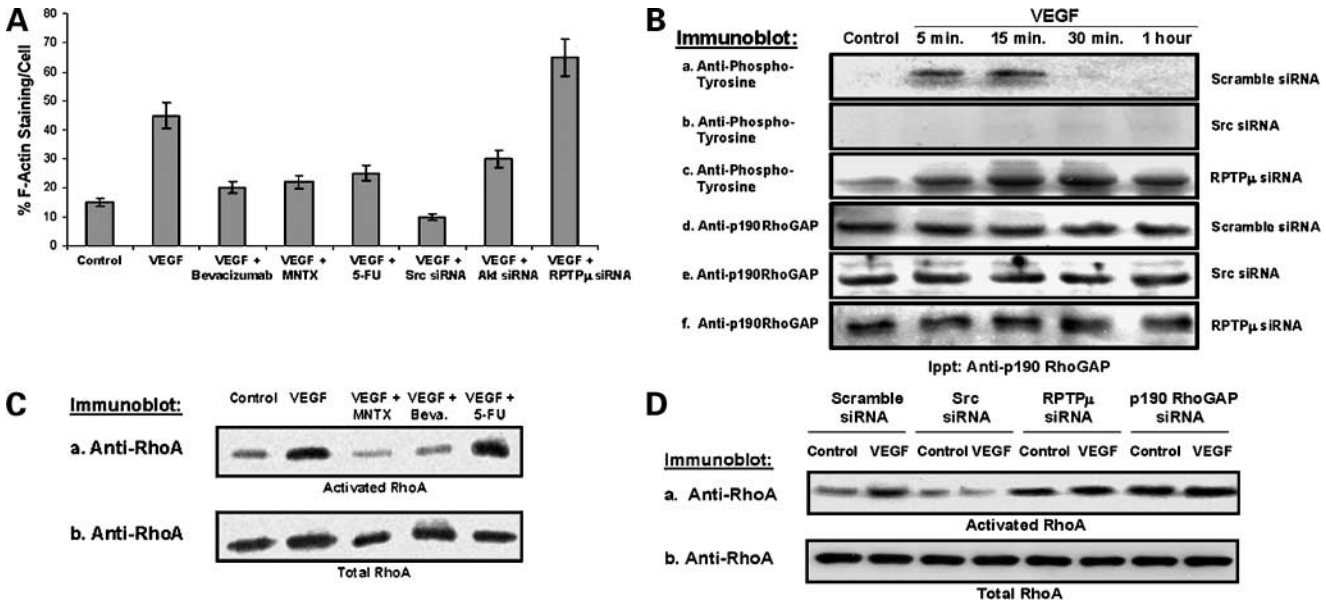

Figure 4. Effects of RPTPμ on VEGF-induced p190 RhoGAP inactivation and MNTX, bevacizumab, and 5-FU regulation of VEGF-induced RhoA activation in human EC. **A,** human EC were either untreated (control) or treated with 100 nmol/L VEGF for 6 h in the presence or absence of pretreatment with bevacizumab (100 ng/mL), MNTX (100 nmol/L), 5-FU (100 μmol/L), Src siRNA, Akt siRNA, or RPTPμ siRNA. EC were then fixed in 4% paraformaldehyde and probed with TRITC-phalloidin and fluorescent images were obtained. Images were analyzed using ImageQuant software. Total F-actin fluorescence intensity per total cell area was calculated for each EC as we have described previously (20). *Y axis,* 50 EC per condition were analyzed. *Bars,* SD. **B,** human EC were serum starved for 1 h and were either untreated (control) or treated with 100 nmol/L VEGF for 5, 15, 30, or 60 min with pretreatment with scramble siRNA (siRNA that does not target any known mRNA sequence), Src siRNA, or RPTPμ siRNA. EC were then solubilized in immunoprecipitation buffer [50 mmol/L HEPES (pH 7.5), 150 mmol/L NaCl, 20 mmol/L $MgCl_2$, 1% NP-40, 0.2 mmol/L phenylmethylsulfonyl fluoride, 1:250 dilution of Calbiochem protease inhibitor mixture 3] and immunoprecipitated with anti-p190 RhoGAP antibody. The resulting immunobeads were run on SDS-PAGE and immunoblotted with anti-phoshotyrosine (*a–c*) or anti-p190 RhoGAP (*d-f*) antibody. Experiments were done in triplicate. Representative data are shown. **C,** human EC were either untreated (control) or treated with VEGF (100 nmol/L, 5 min) with or without pretreatment (1 h) with 100 nmol/L MNTX, 100 ng/mL bevacizumab, or 100 μmol/L 5-FU. EC lysates were obtained, a portion was kept for total RhoA immunoblotting, and the remaining lysate was incubated with Rho-binding domain–conjugated beads. Activated RhoA-bound beads (*a*) or cell lysates (*b*) were run on SDS-PAGE and immunoblotted with anti-RhoA antibody as we have described previously (20, 21). **D,** human EC were either untreated (control) or treated with VEGF (100 nmol/L, 5 min) with pretreatment of either scramble siRNA, Src siRNA, RPTPμ siRNA, or p190 RhoGAP siRNA. EC lysates were obtained, a portion was kept for total RhoA immunoblotting, and the remaining lysate was incubated with Rho-binding domain–conjugated beads. Activated RhoA-bound beads (*a*) or cell lysates (*b*) were run on SDS-PAGE and immunoblotted with anti-RhoA antibody as we have described previously (20, 21).

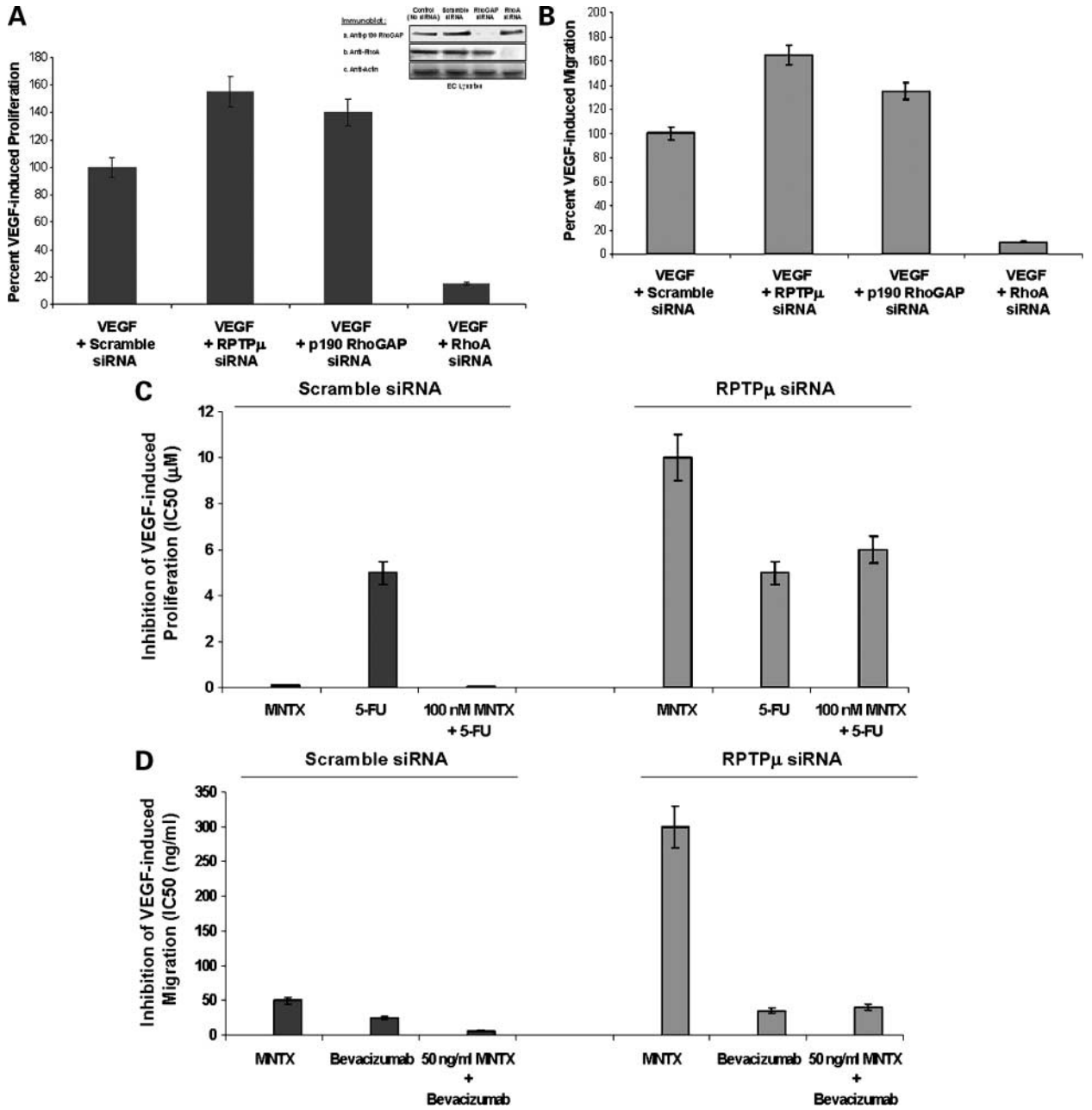

Figure 5. Effect of RPTPμ on MNTX-mediated synergistic effects with bevacizumab and 5-FU on inhibition of VEGF-induced angiogenic events. **A,** graphical representation of human EC assayed for VEGF (100 nmol/L) – induced proliferation (24 h) with pretreatment of either scramble siRNA, RPTPμ siRNA, p190 RhoGAP siRNA, or RhoA siRNA. Experiments were done in triplicate. *Bars,* SD. *Inset,* human EC either untreated (control) or treated with scramble siRNA, p190 RhoGAP siRNA, or RhoA siRNA for 48 h. Lysates were obtained, run on SDS-PAGE, and immunoblotted with anti-p190 RhoGAP (*a*), anti-RhoA (*b*), or anti-actin (*c*) antibody. **B,** graphical representation of human EC assayed for VEGF (100 nmol/L) – induced migration (24 h) with pretreatment of either scramble siRNA, RPTPμ siRNA, p190 RhoGAP siRNA, or RhoA siRNA. Experiments were done in triplicate. *Bars,* SD. **C,** graphical representation of the 50% inhibition concentration (IC_{50}, μmol/L) of MNTX, 5-FU or 100 nmol/L MNTX + 5-FU with pretreatment of scramble siRNA or RPTPμ siRNA of human EC assayed for VEGF (100 nmol/L) – induced proliferation (24 h). Experiments were done in triplicate. *Bars,* SD. **D,** graphical representation of the 50% inhibition concentration (IC_{50}, ng/mL) of MNTX, bevacizumab, or 100 nmol/L MNTX + bevacizumab with pretreatment of scramble siRNA or RPTPμ siRNA of human EC assayed for VEGF (100 nmol/L) – induced migration (24 h). The unit ng/mL was used instead of μmol/L due to the proprietary nature of the molecular weight of bevacizumab. Experiments were done in triplicate. *Bars,* SD.

single and multiple dosing and populations (40). The concentrations of MNTX in our *in vitro* study were similar to those achieved in clinical trials of the drug. In methadone maintenance patients who received mean doses of 0.1 mg/kg MNTX i.v., the mean plasma levels of MNTX were 162 ng/mL. After repeated i.v. doses of MNTX in volunteers, levels of MNTX in plasma were maintained well above the range in which we observed a synergistic

effect with bevacizumab and 5-FU on inhibition of VEGF-induced angiogenic events (41). In a volunteer study of oral MNTX (up to 19.2 mg/kg), mean plasma concentrations of 165 ng/mL with a $t_{1/2}$ of 204 min were recorded (35). Taken as a whole, the plasma concentrations of morphine and MNTX in patients after parenteral or oral administration are consistent with the levels that regulated synergistic inhibition of VEGF-induced angiogenesis and inhibited Src in our *in vitro* model (see Fig. 2). Importantly, we note that the effects of MNTX that occur beyond the VEGF receptor do not appear to be related to its μ-opiate antagonism because naloxone and naltrexone in much higher concentrations do not exert this effect.

We focused our studies on bevacizumab and 5-FU based on their mechanism of action and their common usage. In principle, the synergy we observed could occur with other agents that have the same mechanism. Bevacizumab, a neutralizing antibody to VEGF, was the first U.S. Food and Drug Administration–approved biological therapy designed to inhibit the formation of new blood vessels to tumors. Recently, the Food and Drug Administration approved the use of bevacizumab in first-line treatment of metastatic colorectal cancer when the drug was added to standard chemotherapy (26, 27). Further, a recent breast cancer clinical trial using 722 women who had recurrent or metastatic breast cancer that had not been treated previously with chemotherapy indicated that bevacizumab, in combination with paclitaxel, delayed the progression of disease by an average of ~5 months (25). In addition, patients in a recent lung cancer study receiving a regimen of chemotherapy (paclitaxel and carboplatin) and bevacizumab had a median overall survival of 12.5 months compared with the control group, receiving only paclitaxel and carboplatin, who survived an average of 10.2 months (2). The results of these clinical trials indicate the potential for improved survival rates with the addition of antiangiogeneic therapy. The concentrations we have used in this study are similar to what can be achieved clinically (2, 42). However, there were significant side effects including venous thromboembolism, hypertension, proteinuria, and epistaxis (23–25) and the cost of drug has resulted in use limitation (5).

5-FU is one of the oldest chemotherapy drugs currently in use (44). 5-FU binds to thymidylate synthetase and thereby inhibits cancer cell proliferation (45). Leucovorin enhances the binding of 5-FU to thymidylate synthetase and prolongs the lifespan of 5-FU *in vivo* (44). In addition, 5-FU has been reported to inhibit Akt activation, proliferation, migration, and actin cytoskeletal reorganization of EC, which is consistent with our data (46–48). We are currently examining the exact mechanism(s) by which 5-FU inhibits VEGF-induced Akt activation and actin cytoskeletal dynamics. Although 5-FU has been used to treat numerous cancers, there are significant side effects including diarrhea, nausea, chest pain, and palmar-plantar erythrodysesthesia (28, 44). The degree and severity of the side effects depend on many factors including the dosage of 5-FU (44). Thus, a drug that could potentiate the cellular effects of 5-FU while reducing the dose could be of potential benefit.

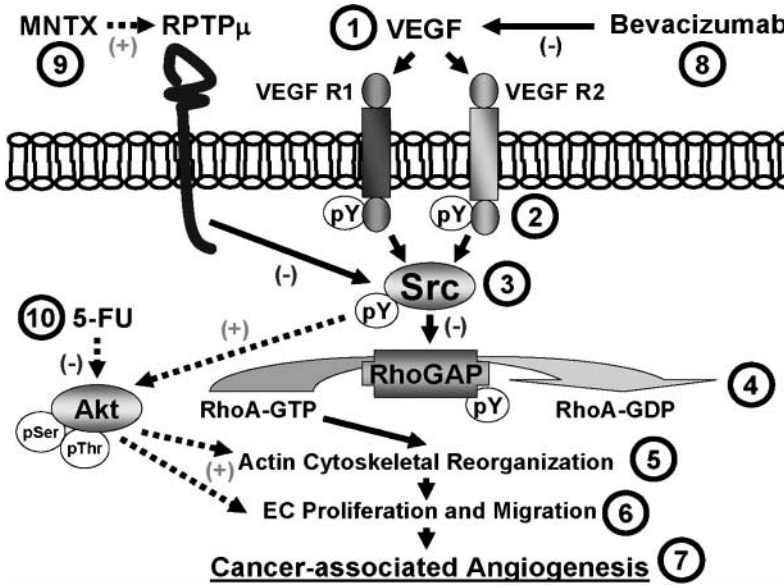

Figure 6. Schematic diagram of a proposed mechanism of MNTX synergistic effects with bevacizumab and 5-FU on inhibition of VEGF-induced angiogenic events. VEGF binding to VEGF receptors (*1*) induces VEGF receptor (*2*) and Src activation (tyrosine phosphorylation; *3*), Src-mediated p190 RhoGAP inactivation (tyrosine phosphorylation; *4*), and consequent RhoA activation (increased GTP-bound form of RhoA). Activated RhoA promotes actin cytoskeletal reorganization (*5*) required for VEGF-induced proliferation and migration (*6*), two key events required for angiogenesis (*7*). Bevacizumab (*8*) inhibits the initial VEGF binding to VEGF receptors. MNTX (*9*) stimulation of RPTPμ activity inhibits VEGF-induced Src activation, Src-mediated p190 RhoGAP inactivation, and consequent RhoA activation. 5-FU (*10*) inhibits VEGF-induced Akt activation (serine/threonine phosphorylation) and actin cytoskeletal reorganization. Therefore, the synergistic effects of MNTX with bevacizumab and 5-FU are achieved through inhibition of different components of a common VEGF-induced angiogenic signaling pathway. MNTX can have important clinical utility by potentially lowering the therapeutic doses of 5-FU and bevacizumab in the treatment of various diseases requiring angiogenesis including cancer.

It has been reported previously that inhibition of Src protects from EC barrier disruption and angiogenesis (8, 9); results are consistent with our data. Src regulates several potential angiogenic events including EC contraction and vascular permeability (9, 49). We extended these findings by observing that Src regulates VEGF-induced Akt activation and actin cytoskeletal regulatory molecules important for EC proliferation and migration. Further, our data suggest that MNTX can inhibit VEGF-mediated Src activation. We therefore examined potential transmembrane proteins (that is, RPTPμ) that can regulate Src activity based on the observations that MNTX, which is charged and cannot easily pass through the plasma membrane of cells, can inhibit Src that is localized to the cytosol and inner leaflet of the plasma membrane (7).

We have observed that RPTPμ plays an important role in inhibiting VEGF-induced angiogenic events. RPTPμ is highly expressed in the vasculature where it is localized to EC junctions (17–19). Consistent with our results, researchers have shown that silencing RPTPμ expression inhibits EC barrier function (19), a prerequisite for angiogenesis. We have extended these findings to show that RPTPμ can regulate VEGF-induced Src activation. We are currently examining the role of these signaling molecules in MNTX-mediated inhibition of angiogenesis. Further, we are exploring whether MNTX can directly bind to RPTPμ or exert its effects on RPTPμ activity indirectly.

Our results indicate that VEGF promotes Src-mediated phosphorylation of p190 RhoGAP. Tyrosine phosphorylation of p190 RhoGAP inactivates its GTPase activity resulting in increased active (GTP-bound) RhoA (13, 14). The active form (GTP-bound) of RhoA can bind to and activate several important downstream signaling molecules including the serine/threonine kinases ROCK, PKN1, PAK-2, and CRIK (50). The role of these kinases in opiate-induced angiogenesis is currently under investigation in our laboratory.

Although there are obvious caveats to extending our results to practice, our observations that MNTX acts synergistically with bevacizumab and 5-FU on inhibition of VEGF-induced angiogenic events are intriguing and could have clinical implications. First, because we have shown previously that morphine and other opiates at therapeutic doses enhanced EC migration and proliferation (6), MNTX treatment may have an additional benefit for patients taking regular doses of opiates for tumor-associated pain. In addition, MNTX could attenuate the effects of endogenous opioids that are released in stress or pain. An effect of these endogenous opioids on tumor growth has been postulated. Finally, the synergy of MNTX with antiangiogenic therapies indicates that MNTX could facilitate dose reduction of these agents. Therefore, further studies are warranted.

Disclosure of Potential Conflicts of Interest

J. Moss: Progenics Pharmaceuticals consultant, has a financial interest in MNTX as a patent holder through the University of Chicago, and receives stock options from Progenics Pharmaceuticals. The other authors disclosed no potential conflicts of interest.

References

1. Larkin JM, Chowdhury S, Gore ME. Drug insight: advances in renal cell carcinoma and the role of targeted therapies. Nat Clin Pract Oncol 2007;4:470–9.

2. Cohen MH, Gootenberg J, Keegan P, Pazdur R. FDA drug approval summary: bevacizumab (Avastin) plus carboplatin and paclitaxel as first-line treatment of advanced/metastatic recurrent nonsquamous non-small cell lung cancer. Oncologist 2007;12:713–8.

3. Emmanouilides C, Sfakiotaki G, Androulakis N, et al. Front-line bevacizumab in combination with oxaliplatin, leucovorin and 5-fluorouracil (FOLFOX) in patients with metastatic colorectal cancer: a multicenter phase II study. BMC Cancer 2007;7:91.

4. Jansman FG, Postma MJ, Brouwers JR. Cost considerations in the treatment of colorectal cancer. Pharmacoeconomics 2007;25:537–62.

5. Kolesar JM. Bevacizumab: improved survival at what cost? Am J Health Syst Pharm 2005;62:1017.

6. Singleton PA, Lingen MW, Fekete MJ, Garcia JGN, Moss J. Methylnaltrexone inhibits opiate and VEGF-induced angiogenesis: role of receptor transactivation. Microvasc Res 2006;72:3–11.

7. Alper O, Bowden ET. Novel insights into c-Src. Curr Pharm Des 2005;11:1119–30.

8. Weis S, Cui J, Barnes L, Cheresh D. Endothelial barrier disruption by VEGF-mediated Src activity potentiates tumor cell extravasation and metastasis. J Cell Biol 2004;167:223–9.

9. Mucha DR, Myers CL, Schaeffer RC, Jr. Endothelial contraction and monolayer hyperpermeability are regulated by Src kinase. Am J Physiol Heart Circ Physiol 2003;284:H994–1002.

10. Hoang MV, Whelan MC, Senger DR. Rho activity critically and selectively regulates endothelial cell organization during angiogenesis. Proc Natl Acad Sci U S A 2004;101:1874–9.

11. Liu Y, Senger DR. Matrix-specific activation of Src and Rho initiates capillary morphogenesis of endothelial cells. FASEB J 2004;18:457–68.

12. Hakoshima T, Shimizu T, Maesaki R. Structural basis of the Rho GTPase signaling. J Biochem (Tokyo) 2003;134:327–31.

13. Chang JH, Gill S, Settleman J, Parsons SJ. c-Src regulates the simultaneous rearrangement of actin cytoskeleton, p190RhoGAP, and p120RasGAP following epidermal growth factor stimulation. J Cell Biol 1995;130:355–68.

14. Roof RW, Dukes BD, Chang JH, Parsons SJ. Phosphorylation of the p190 RhoGAP N-terminal domain by c-Src results in a loss of GTP binding activity. FEBS Lett 2000;472:117–21.

15. Croft DR, Sahai E, Mavria G, et al. Conditional ROCK activation *in vivo* induces tumor cell dissemination and angiogenesis. Cancer Res 2004;64:8994–9001.

16. Stoker AW. Protein tyrosine phosphatases and signalling. J Endocrinol 2005;185:19–33.

17. Koop EA, Lopes SM, Feiken E, et al. Receptor protein tyrosine phosphatase μ expression as a marker for endothelial cell heterogeneity; analysis of RPTPμ gene expression using LacZ knock-in mice. Int J Dev Biol 2003;47:345–54.

18. Aricescu AR, Hon WC, Siebolt C, Lu W, van der Merwe PA, Jones EY. Molecular analysis of receptor protein tyrosine phosphatase μ-mediated cell adhesion. EMBO J 2006;25:701–12.

19. Sui XF, Kiser TD, Hyun SW, et al. Receptor protein tyrosine phosphatase micro regulates the paracellular pathway in human lung microvascular endothelia. Am J Pathol 2005;166:1247–58.

20. Singleton PA, Dudek SM, Ma SF, Garcia JGN. Transactivation of sphingosine 1-phosphate receptors is essential for vascular barrier regulation. Novel role for hyaluronan and CD44 receptor family. J Biol Chem 2006;281:34381–93.

21. Singleton PA, Moreno-Vinasco L, Sammani S, Wanderling SL, Moss J, Garcia JGN. Attenuation of vascular permeability by methylnaltrexone: role of mOP-R and S1P3 transactivation. Am J Respir Cell Mol Biol 2007;37:222–31.

22. Garcia JGN, Liu F, Verin AD, et al. Sphingosine 1-phosphate promotes endothelial cell barrier integrity by Edg-dependent cytoskeletal rearrangement. J Clin Invest 2001;108:689–01.

23. Gupta K, Zhang J. Angiogenesis: a curse or cure? Postgrad Med J 2005;81:236–42.

24. Glade-Bender J, Kandel JJ, Yamashiro DJ. VEGF blocking therapy in the treatment of cancer. Expert Opin Biol Ther 2003;3:263 – 76.

25. Widakowich C, de Azambuj E, Gil T, et al. Molecular targeted therapies in breast cancer: where are we now? Int J Biochem Cell Biol 2007;39:1375 – 87.

26. Hurwitz H, Saini S. Bevacizumab in the treatment of metastatic colorectal cancer: safety profile and management of adverse events. Semin Oncol 2006;33:S26 – 34.

27. Hurwitz H, Kabbinavar, F. Bevacizumab combined with standard fluoropyrimidine-based chemotherapy regimens to treat colorectal cancer. Oncology 2005;69 Suppl 3:17 – 24.

28. El-Khoueiry AB, Lenz HJ. Should continuous infusion 5-fluorouracil become the standard of care in the USA as it is in Europe? Cancer Invest 2006;24:50 – 5.

29. Bourguignon LY, Singleton PA, Zhu H, Diedrich F. Hyaluronan-mediated CD44 interaction with RhoGEF and Rho kinase promotes Grb2-associated binder-1 phosphorylation and phosphatidylinositol 3-kinase signaling leading to cytokine (macrophage-colony stimulating factor) production and breast tumor progression. J Biol Chem 2003;278:29420 – 34.

30. Moss J, Foss J. Pain relief without side effects: peripheral opiate antagonists. Vol. 33. Philadelphia: Lippincott Williams & Wilkins; 2005. p. 175 – 86.

31. Hoskin PJ, Hanks GW. Opioid agonist-antagonist drugs in acute and chronic pain states. Drugs 1991;41:326 – 44.

32. Greenwood-Van Meerveld B, Gardner CJ, Little PJ, Hicks GA, Dehaven-Hudkins DL. Preclinical studies of opioids and opioid antagonists on gastrointestinal function. Neurogastroenterol Motil 2004;16 Suppl 2: 46 – 53.

33. Sykes NP. Using oral naloxone in management of opioid bowel dysfunction. New York: Haworth Medical Press; 2005. p. 175 – 95.

34. Yuan CS, Foss JF, O'Connor M, et al. Methylnaltrexone for reversal of constipation due to chronic methadone use: a randomized controlled trial. JAMA 2000;283:367 – 72.

35. Yuan CS. Clinical status of methylnaltrexone, a new agent to prevent and manage opioid-induced side effects. J Support Oncol 2004;2:111 – 7; discussion 119 – 22.

36. Yuan CS, Foss JF, Moss J. Effects of methylnaltrexone on morphine-induced inhibition of contraction in isolated guinea-pig ileum and human intestine. Eur J Pharmacol 1995;276:107 – 11.

37. Yuan CS. Methylnaltrexone mechanisms of action and effects on opioid bowel dysfunction and other opioid adverse effects. Ann Pharmacother 2007;41:984 – 93.

38. Stanski DR, Greenblatt DJ, Lowenstein E. Kinetics of intravenous and intramuscular morphine. Clin Pharmacol Ther 1978;24:52 – 9.

39. Neumann PB, Henriksen H, Grosman N, Christensen CB. Plasma morphine concentrations during chronic oral administration in patients with cancer pain. Pain 1982;13:247 – 52.

40. Collins SL, Faura CC, Moore RA, McQuay HJ. Peak plasma concentrations after oral morphine: a systematic review. J Pain Symptom Manage 1998;16:388 – 02.

41. Yuan CS, Doshan H, Charney MR, et al. Tolerability, gut effects, and pharmacokinetics of methylnaltrexone following repeated intravenous administration in humans. J Clin Pharmacol 2005;45:538 – 46.

42. Cabebe E, Wakelee H. Role of anti-angiogenesis agents in treating NSCLC: focus on bevacizumab and VEGFR tyrosine kinase inhibitors. Curr Treat Options Oncol 2007;81:15 – 27.

43. Kramer I, Lipp HP. Bevacizumab, a humanized anti-angiogenic monoclonal antibody for the treatment of colorectal cancer. J Clin Pharm Ther 2007;32:1 – 14.

44. Longley DB, Harkin DP, Johnston PG. 5-Fluorouracil: mechanisms of action and clinical strategies. Nat Rev Cancer 2003;3:330 – 8.

45. Danenberg PV. Pharmacogenomics of thymidylate synthase in cancer treatment. Front Biosci 2004;9:2484 – 94.

46. Gordon SR, Climie M, Hitt A. L. 5-Fluorouracil interferes with actin organization, stress fiber formation and cell migration in corneal endothelial cells during wound repair along the natural basement membrane. Cell Motil Cytoskeleton 2005;62:244 – 58.

47. Basaki Y, Chikahisa L, Aoyagi K, et al. γ-Hydroxybutyric acid and 5-fluorouracil, metabolites of UFT, inhibit the angiogenesis induced by vascular endothelial growth factor. Angiogenesis 2001;4:163 – 73.

48. Islam S, Hassan F, Tumurkhuu G, et al. 5-Fluorouracil prevents lipopolysaccharide-induced nitric oxide production in RAW 264.7 macrophage cells by inhibiting Akt-dependent nuclear factor-κB activation. Cancer Chemother Pharmacol 2007;59:227 – 33.

49. Chen R, Kim O, Yang J, et al. Regulation of Akt/PKB activation by tyrosine phosphorylation. J Biol Chem 2001;276:31858 – 62.

50. Fujisawa K, Madaule P, Ishizaki T, et al. Different regions of Rho determine Rho-selective binding of different classes of Rho target molecules. J Biol Chem 1998;273:18943 – 49.

Molecular Cancer Therapeutics

Synergistic effects of methylnaltrexone with 5-fluorouracil and bevacizumab on inhibition of vascular endothelial growth factor–induced angiogenesis

Patrick A. Singleton, Joe G.N. Garcia and Jonathan Moss

Mol Cancer Ther 2008;7:1669-1679.